

# [Cp\*Fe( $\eta^5$ -P<sub>5</sub>)] as a Useful Source for the Synthesis of Cobalt Complexes with “Naked” P<sub>n</sub> Ligands

Otto J. Scherer,\* Sascha Weigel, and Gotthelf Wolmershäuser

Dedicated to Professor Peter Jutzli on the occasion of his 60th birthday

**Abstract:** The cothermolysis of the sandwich complex [Cp\*Fe( $\eta^5$ -P<sub>5</sub>)] (**1**) and [Cp<sup>R</sup>Co(CO)<sub>2</sub>] (**2a**: Cp<sup>R</sup> = C<sub>5</sub>H<sub>4</sub>tBu, **2b**: Cp<sup>R</sup> = C<sub>5</sub>H<sub>3</sub>tBu<sub>2</sub>-1,3) gives the following series of clusters with “naked” P<sub>n</sub> ligands: [[Cp\*Fe]{Cp<sup>R</sup>CoP<sub>4</sub>}-{FeCp\*}] (**4**), a “triple decker” with a CoP<sub>4</sub> middle deck, [[Cp\*Fe]{Cp<sup>R</sup>Co}<sub>2</sub>-(P<sub>4</sub>)(P)] (**5**), [[Cp<sup>R</sup>Co]<sub>4</sub>P<sub>4</sub>] (**6a**, **b**), and [[Cp<sup>R</sup>Co]<sub>3</sub>( $\mu_3$ -P)<sub>2</sub>] (**7a**, **b**). The thermal or photochemical reaction of [Cp\*Fe( $\eta^5$ -P<sub>5</sub>)] (**1**) (Cp\* = C<sub>5</sub>Me<sub>4</sub>Et)

with [[Cp<sup>R</sup>Co( $\mu$ -CO)]<sub>2</sub>] (**3**) (Cp<sup>R</sup> = C<sub>5</sub>H<sub>3</sub>tBu<sub>2</sub>-1,3) affords [[Cp\*Fe]( $\mu_4$ - $\eta^5$ : $\eta^2$ : $\eta^2$ : $\eta^1$ -P<sub>5</sub>){Co(CO)Cp<sup>R</sup>}{Co<sub>2</sub>Cp<sup>R</sup><sub>2</sub>( $\mu$ -CO)}] (**8**) in which, in addition to the  $\eta^5$ -cyclo-P<sub>5</sub> coordination, one terminal and two  $\eta^2$  side-on binding coordination modes have been realized. In the case of the cubanelike compounds **6a** and **6b**

the oxidation of its P atoms with S<sub>8</sub> or Se<sub>(grey)</sub> gives [[Cp<sup>R</sup>Co]<sub>4</sub>(P)(PX)<sub>3</sub>] (**9**: X = S, **10**: X = Se; Cp<sup>R</sup> = C<sub>5</sub>H<sub>4</sub>tBu), products of threefold oxidation, and [[Cp<sup>R</sup>Co]<sub>4</sub>-(P)<sub>2</sub>(PX)<sub>2</sub>] (**12**: X = S, **13**: X = Se; Cp<sup>R</sup> = C<sub>5</sub>H<sub>3</sub>tBu<sub>2</sub>-1,3) with only two PX ligands. [[Cp<sup>R</sup>Co]<sub>4</sub>( $\mu_3$ -PS)<sub>4</sub>] (**11**), the fully sulfurized derivative of **6a**, can be synthesized by oxidation of **9** with S<sub>8</sub> in dichloromethane. The complexes **4**, **5**, **6b**, **7b**, **8**, and **10** have been characterized by X-ray crystal structure determination.

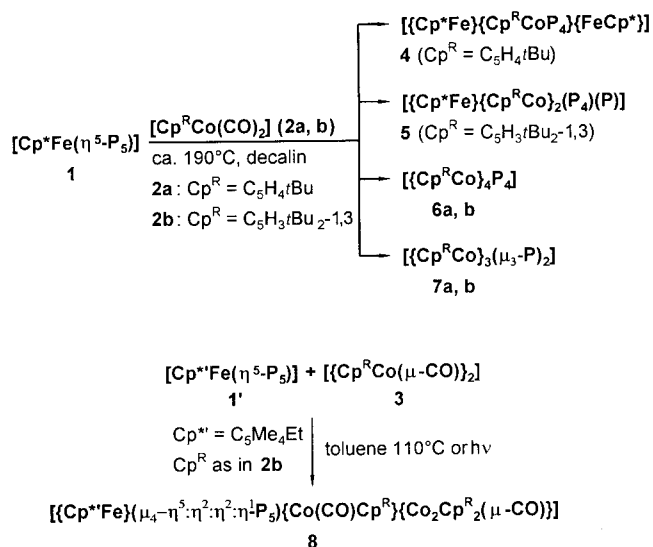
**Keywords:** clusters • cobalt • iron • P ligands • PS/PSe ligands

## Introduction

The successful synthesis of [Cp\*Fe( $\eta^5$ -P<sub>5</sub>)] (**1**), the first sandwich complex with the isoelectronic all-phosphorus analogue of C<sub>5</sub>H<sub>5</sub><sup>-</sup> as a complex ligand,<sup>[1]</sup> opened an interesting aspect on the novel chapter of complexes with naked P<sub>n</sub> ligands.<sup>[2]</sup> Since 1987 it has been shown that compound **1** is a versatile starting material for rather different products with substituent-free phosphorus ligands. Besides its stacking reaction to a cationic 30 valence electron (VE) triple decker,<sup>[3]</sup> reactions are known in which the P<sub>5</sub> ring remains intact<sup>[4]</sup> or is cleaved with formation of a P<sub>5</sub> chain,<sup>[4]</sup> P<sub>4</sub>/P<sub>1</sub>, P<sub>3</sub>/P<sub>2</sub>, or P<sub>2</sub> fragments.<sup>[4–6]</sup> The unusual  $\eta^5$ : $\eta^2$  coordination mode of the cyclo-P<sub>5</sub> ligand has also been described.<sup>[1c]</sup>

## Results and Discussion

The cothermolysis of [Cp\*Fe( $\eta^5$ -P<sub>5</sub>)] (**1**) and the mononuclear cobalt complexes [Cp<sup>R</sup>Co(CO)<sub>2</sub>] (**2a,b**) at 190 °C in decalin affords the multinuclear complexes **4–7** listed in Scheme 1,



Scheme 1. Reaction schemes for the formation of compounds **4–8**.

besides small amounts of [[Cp\*Fe]<sub>2</sub>( $\mu$ - $\eta^2$ : $\eta^2$ -P<sub>2</sub>)<sub>2</sub>]<sup>[7]</sup> and [[Cp<sup>R</sup>Co]<sub>2</sub>( $\mu$ - $\eta^2$ : $\eta^2$ -P<sub>2</sub>)<sub>2</sub>]<sup>[8]</sup> detected by <sup>31</sup>P NMR spectroscopy. With the dinuclear cobalt compound **3** the photochemical or thermal reaction with **1** leads to **8**, a tetranuclear cluster with an intact cyclo-P<sub>5</sub> ligand forming the hitherto unknown  $\mu_4$ - $\eta^5$ : $\eta^2$ : $\eta^2$ : $\eta^1$  coordination mode.

The impact of small changes of the substituent pattern for the Cp<sup>R</sup> ligand on the Co atom can nicely be inferred from

[\*] Prof. Dr. O. J. Scherer, Dipl. Chem. S. Weigel, Dr. G. Wolmershäuser<sup>[†]</sup>  
 Fachbereich Chemie der Universität, Erwin-Schrödinger-Strasse  
 D-67663 Kaiserslautern (Germany)  
 Fax: (+49) 631-205-2187  
 E-mail: oscherer@rhrk.uni-kl.de

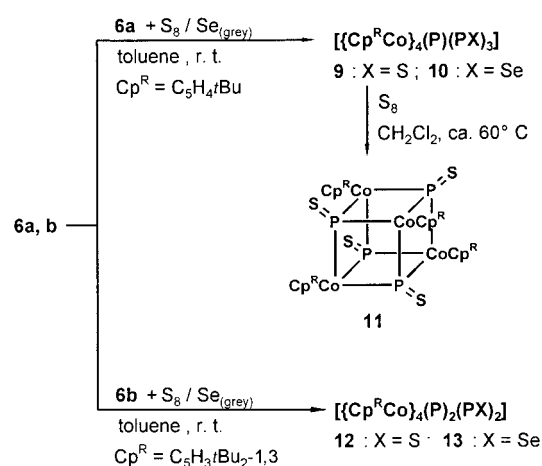
[†] X-ray crystal structure determinations

Scheme 1. In the case of **2a** ( $\text{Cp}^{\text{R}} = \text{C}_5\text{H}_4t\text{Bu}$ ), reaction with **1** gives, besides **6a** and **7a**, the triple decker  $[[\text{Cp}^{\text{R}}\text{Fe}]\{\text{Cp}^{\text{R}}\text{CoP}_4\}\{\text{FeCp}^{\text{R}}\}]$  (**4**) with the hitherto unknown five-membered  $\text{CoP}_4$  middle deck. The same reaction with **2b** ( $\text{Cp}^{\text{R}} = \text{C}_5\text{H}_3t\text{Bu}_{2-1,3}$ ) with an additional *tert*-butyl group in the Cp ring, gives the compound  $[[\text{Cp}^{\text{R}}\text{Fe}]\{\text{Cp}^{\text{R}}\text{Co}_2(\text{P}_4)(\text{P})\}]$  (**5**), a cubanelike cluster with an  $\text{FeCo}_2\text{P}_5$  skeleton, as well as **6b** and **7b**. The  $\text{P}_5$  part of **5** consists of a  $\text{P}_1$  and a tripodal (trigonal pyramidal)  $\text{P}_4$  ligand, which can be derived formally from the  $\text{P}_4$  tetrahedron by cleaving three of its six P–P bonds.

If the mononuclear cobalt complex **2b** is replaced by the dinuclear species **3**, reaction with **1'** (Scheme 1) affords exclusively  $[[\text{Cp}^{\text{R}}\text{Fe}](\mu_4\text{-}\eta^5\text{-}\eta^2\text{-}\eta^1\text{-}\text{P}_5)\{\text{Co}(\text{CO})\text{Cp}^{\text{R}}\}\{\text{Co}_2\text{Cp}^{\text{R}}(\mu\text{-CO})\}]$  (**8**) with the remarkable  $\mu_4\text{-}\eta^5\text{-}\eta^2\text{-}\eta^1$  coordination mode of the cyclo- $\text{P}_5$  ligand (for details, see discussion of the X-ray crystal structures). Compounds **4–8** are slightly air sensitive. Crystals of dark green **7a, b**, red-brown **9, 10, 11, 12, 13** (Scheme 2), brown-black **4**, and grey-metallic **5** are poorly soluble in hexane, but dissolve easily in toluene and still better in dichloromethane (**6a, b** and **8** are also readily soluble in hexane).

**Oxidation of  $[[\text{Cp}^{\text{R}}\text{Co}]_4\text{P}_4]$  (**6a, b**) with  $\text{S}_8$  and  $\text{Se}_{(\text{grey})}$ :** Since the discovery of the first complex with a  $\mu_3\text{-PO}$  ligand in 1991,<sup>[9a]</sup> growing interest for the coordinative stabilisation of PX ligands ( $\text{X} = \text{O}^{[9]}$ ,  $\text{S}^{[10]}$ ,  $\text{Se}^{[11]}$ ) has emerged. Starting with the tetranuclear complexes **6a** and **6b**, oxidation products have been realized from the reaction with  $\text{S}_8$  or  $\text{Se}_{(\text{grey})}$  (Scheme 2).

It is worthwhile mentioning that in **6a** ( $\text{Cp}^{\text{R}} = \text{C}_5\text{H}_4t\text{Bu}$ ) three of the four P ligands can be oxidized by sulfur ( $\text{S}_8$ ) or grey selenium with formation of the complexes **9** and **10**. In dichloromethane instead of toluene, **9** reacts further with  $\text{S}_8$  to the fully oxidized cubanelike compound **11** with four  $\mu_3\text{-PS}$  ligands. Only double oxidation is observed on the sulfurization and selenization of **6b** ( $\text{Cp}^{\text{R}} = \text{C}_5\text{H}_3t\text{Bu}_{2-1,3}$ ) giving **12** and **13**.



Scheme 2. Reaction scheme for the oxidation of **6a** and **6b**.

**NMR Spectra of the complexes 4–13:**  $^1\text{H}$  and  $^{31}\text{P}$  NMR data are summarized in Table 1. A characteristic low-field shift of the  $^{31}\text{P}$  NMR signal was found for all compounds in which one or more P atoms are surrounded by three  $\text{L}_n\text{M}$ -complex fragments. The values of  $\delta = 1047$  and  $1059$  in  $[[\text{Cp}^{\text{R}}\text{Co}]_3(\mu_3\text{-P})_2]$  (**7a, b**) do not differ significantly from  $\delta(\mu_3\text{-P}) = 913$  in  $[[\text{L}(\text{OC})_2\text{Fe}]_3(\mu_3\text{-P})(\mu_4\text{-P})\{\text{Mn}(\text{CO})_2\text{Cp}\}]$  (**14**)<sup>[12]</sup> [ $\text{L} = \text{P}(\text{OC}_3\text{H}_7\text{-}i)_3$ ]. It is noteworthy that for the phosphorus atoms of the  $\text{CoP}_4$  middle deck in the triple decker **4** (Scheme 1) the signals are deshielded to  $\delta = 938$  and  $564$ . In cubanelike  $[[\text{Cp}^{\text{R}}\text{Ta}]_2[\text{Cp}^{\text{R}}\text{Fe}](\text{P}_4)(\text{P})]$  (**15**)<sup>[5]</sup> as in  $[[\text{Cp}^{\text{R}}\text{Fe}]\{\text{Cp}^{\text{R}}\text{Co}_2(\text{P}_4)(\text{P})\}]$  (**5**) ( $\text{Cp}^{\text{R}} = \text{C}_5\text{H}_3t\text{Bu}_{2-1,3}$  for both molecules) the P atom on the top of the  $\text{P}_4$  pyramid has  $^{31}\text{P}$  NMR signals (**5**:  $\delta = -208$ , **15**:  $\delta = -313$ ) at rather high field. In the series **6a/11** ( $^{31}\text{P}$   $\delta = 484/238$ ) the phosphorus NMR signals show the same trend, which was also observed on going from the cubane  $[(\text{RC})_4\text{P}_4]$  to the fully sulfurized derivative  $[(\text{RC})_4(\text{PS})_4]$  ( $^{31}\text{P}$   $\delta = 257/19$ ;  $\text{R} = t\text{Bu}$ ).<sup>[13]</sup>

**Crystal and molecular structures of the complexes 4, 5, 6b, 7b, 8, and 10:** The crystallographic data for complexes **4, 5, 6b, 7b, 8, and 10**:

Table 1.  $^1\text{H}$  and  $^{31}\text{P}$  NMR data of **4–13** ( $J$  in Hz).

	$^1\text{H}(\text{C}_6\text{D}_6, \text{TMS int.}, 200 \text{ MHz})^{[a]}$ $\delta \text{Cp}^{\text{R}[b]}$	$^{31}\text{P}(\text{C}_6\text{D}_6, 85\% \text{ H}_3\text{PO}_4 \text{ ext.}, 81 \text{ MHz})^{[a]}$ $\delta \text{P}$
<b>4</b>	5.50 (s, 2H), 4.48 (s, 2H), 1.69 (s, 9H), 1.52 (s, 30H)	938 (d, 2P, $^1J(\text{P,P}) = -120$ ), 567 (d, 2P, $^1J(\text{P,P}) = -120$ )
<b>5</b>	5.11 (s, 2H), 4.87 (s, 2H), 4.61 (s, 2H), 1.77 (s, 18H), 1.31 (s, 15H), 1.23 (s, 18H)	562 (s, 1P), 467 (d, 1P, $^1J(\text{P,P}) = -76.3$ ), 354 (d, 2P, $^1J(\text{P,P}) = -198.4$ ), $-208$ (m, 1P)
<b>6a</b>	5.03 (s, 8H), 4.95 (s, 8H), 1.27 (s, 36H)	483.9 (s, 4P)
<b>6b</b>	5.47 (s, 8H), 4.16 (s, 4H), 1.47 (s, 72H)	472.5 (s, 4P)
<b>7a</b>	4.44 (s, 6H), 4.36 (s, 6H), 1.25 (s, 27H)	1046.9 (s, 2P)
<b>7b</b>	4.05 (s, 9H), 1.47 (s, 54H)	1058.7 (s, 2P)
<b>8</b>	5.13 (s, 3H), 5.04 (s, 2H), 4.97 (s, 1H), 4.30 (s, 1H), 4.05 (s, 2H), 2.38 (q, 2H, $^3J(\text{H,H}) = 7.4$ ), 1.78 (s, 9H), 1.68 (s, 9H), 1.51 (s, 9H), 1.49 (s, 9H), 1.47 (s, 9H), 1.45 (s, 9H), 1.35 (s, 12H), 0.99 (t, 3H, $^3J(\text{H,H}) = 7.4$ )	355.0 (pt, 1P, $^1J(\text{P,P}) = -217.5$ ), 212.6 (dt, 1P, $^1J(\text{P,P}) = -535.1$ ), 98 (dd, 1P, $^1J(\text{P,P}) = -512.6$ ), 36 (dd, 1P, $^1J(\text{P,P}) = -434.1$ , $^2J(\text{P,P}) = 31.9$ ), $-5$ (dd, 1P, $^1J(\text{P,P}) = -190.6$ )
<b>9</b>	5.79 (s, 1H), 5.17 (s, 2H), 4.71 (s, 2H), 4.55 (s, 1H), 4.30 (s, 1H), 3.99 (s, 1H), 1.78 (s, 9H), 1.56 (s, 9H), 1.29 (s, 18H)	481.2 (t, 1P, $^2J(\text{P,P}) = 91.8$ ), 271.5 (t, 1P, $^2J(\text{P,P}) = 158$ ), 254.1 (dd, 2P, $^2J(\text{P,P}) = 158$ )
<b>10</b>	5.75 (s, 1H), 5.19 (s, 2H), 4.79 (s, 1H), 4.62 (s, 1H), 4.49 (s, 1H), 4.23 (s, 1H), 4.05 (s, 1H), 1.84 (s, 9H), 1.54 (s, 9H), 1.29 (s, 18H)	486.1 (t, 1P, $^2J(\text{P,P}) = 88.5$ ), 238.8 (t, 1P, $^2J(\text{P,P}) = 155$ , $^1J(\text{P,Se}) = -732.4 / -640.9$ ), 220.0 (dd, 2P, $^2J(\text{P,P}) = 155$ )
<b>11</b>	4.91 (t, 8H), 4.54 (t, 8H, $^2J(\text{H,H}) = 2.1$ ), 1.65 (s, 36H)	238.2 (s, 4P)
<b>12</b>	5.50 (s, 2H), 5.48 (s, 2H), 4.30 (s, 4H), 4.25 (s, 4H), 1.59 (s, 36H), 1.50 (s, 36H)	538.4 (t, 2P, $^2J(\text{P,P}) = 93.4$ ), 230.0 (t, 2P, $^2J(\text{P,P}) = 93.4$ )
<b>13</b>	5.30 (s, 2H), 5.28 (s, 2H), 4.25 (s, 4H), 4.22 (s, 4H), 1.40 (s, 36H), 1.26 (s, 36H)	537.9 (d, 2P, $^2J(\text{P,P}) = 173$ ), 189.4 (d, 2P, $^1J(\text{P,Se}) = -673.6$ )

[a] WP-200 (Bruker), s = broad singlet (multiplet fine structure not resolved), pt = pseudo triplet, [b]  $\text{Cp}^{\text{R}} = \text{C}_5\text{H}_4t\text{Bu}$ : **4, 6a, 7a, 9, 10, 11** and  $\text{Cp}^{\text{R}} = \text{C}_5\text{H}_3t\text{Bu}_{2-1,3}$ : **5, 6b, 7b, 8, 12, 13**.

**8**, **10** are compiled in Table 2. Table 3 contains selected bond lengths and angles for **4**, **8**, and **7b**. Bond distances and angles for complexes **5**, **6b**, and **10** are summarized in Tables 4 and 5.

$[[\text{Cp}^*\text{Fe}][\text{Cp}^R\text{CoP}_4][\text{FeCp}^*]]$  (**4**;  $\text{Cp}^R = \text{C}_5\text{H}_4\text{tBu}$ ): The X-ray crystal structure shows the molecule to be a triple decker with a planar  $\text{CoP}_4$  five-membered ring as middle deck (sum of bond angles =  $540^\circ$ ; smallest angle at  $\text{Co1} = 98.8^\circ$ ). The planes of the two  $\text{Cp}^*$  ligands form an interplanar angle of  $17.7^\circ$  (Figure 1). The angles  $\text{Cp}_{(\text{cent})}^*\text{-Fe1-Fe2}$  and  $\text{Cp}_{(\text{cent})}^*\text{-Fe2-Fe1}$  ( $172.4^\circ$  and  $171.9^\circ$ , respectively) deviate slightly from linearity. Possibly, the sterically demanding  $\text{Cp}^R$  ligand on the Co atom of the  $\text{CoP}_4$  ring plays an important role. The bonds

lengths of the heteroatom ring show the following trend: With a mean value of  $2.18 \text{ \AA}$  the bond lengths  $\text{P1-P2}$  and  $\text{P3-P4}$  are slightly longer than  $\text{P2-P3}$  ( $2.135 \text{ \AA}$ ; Table 3). The average of  $\text{Co1-P1}$  and  $\text{Co1-P4}$  is  $2.16 \text{ \AA}$  and does not differ significantly from  $2.20 \text{ \AA}$   $\text{P3-Co1(1')}$  found in the cubanelike complex **5** (see Table 4 and Figure 5). To the best of our knowledge, **4** is the first triple decker to be realized in which the five-membered middle deck consists of a transition metal complex fragment and four pnictogen atoms. According to the electron-counting rules<sup>[14]</sup> of Wade–Mingos this 30 VE compound<sup>[15]</sup> is a close cluster with  $(n+1)$  skeleton electron pairs (SEP). This is in accordance with the pentagonal bipyramidal  $\text{Fe}_2\text{CoP}_4$  skeleton of **4**.

Table 2. Crystallographic data for complexes **4**, **5**, **6b**, **7b**, **8**, and **10**.

	<b>4</b>	<b>5</b>	<b>6b</b>	<b>7b</b>	<b>8</b>	<b>10</b>
formula	$\text{C}_{29}\text{H}_{43}\text{CoFe}_2\text{P}_4$	$\text{C}_{36}\text{H}_{57}\text{Co}_2\text{FeP}_5$	$\text{C}_{52}\text{H}_{84}\text{Co}_4\text{P}_4$	$\text{C}_{39}\text{H}_{63}\text{Co}_3\text{P}_2$	$\text{C}_{52}\text{H}_{80}\text{Co}_3\text{FeO}_2\text{P}_5$	$\text{C}_{36}\text{H}_{52}\text{Co}_4\text{P}_4\text{Se}_3$
$M_r$	686.1	818.4	1068.8	770.6	1124.65	1081.3
crystal size [mm]	$0.52 \times 0.32 \times 0.18$	$0.32 \times 0.12 \times 0.08$	$0.44 \times 0.24 \times 0.12$	$0.40 \times 0.16 \times 0.05$	$0.68 \times 0.52 \times 0.17$	$0.40 \times 0.30 \times 0.20$
crystal system	monoclinic	orthorhombic	triclinic	monoclinic	monoclinic	monoclinic
space group	$P2_1/n$	$Pnma$	$P\bar{1}$	$C2/c$	$P2_1/n$	$P2_1/n$
$a[\text{\AA}]$	8.4824(6)	12.1278(5)	12.1182(9)	18.5187(12)	19.8339(13)	12.6230(10)
$b[\text{\AA}]$	21.754(2)	20.6671(13)	12.2632(9)	19.3530(13)	12.6626(6)	13.2880(10)
$c[\text{\AA}]$	16.7792(12)	15.8291(7)	20.947(2)	11.5692(7)	22.4571(15)	25.229(3)
$\alpha[^\circ]$	90	90	99.525(8)	90	90	90
$\beta[^\circ]$	95.640(7)	90	91.561(8)	95.828(8)	95.526(7)	104.410(10)
$\gamma[^\circ]$	90	90	115.890(7)	90	90	90
$V[\text{\AA}^3]$	3081.2(4)	3967.5(3)	2744.4(3)	4124.9(5)	5613.9(6)	4098.6(7)
$Z$	4	4	2	4	4	4
$\rho_{\text{calcd}} [\text{g cm}^{-3}]$	1.479	1.370	1.293	1.241	1.331	1.751
$\mu [\text{mm}^{-1}]$	1.686	1.412	1.336	1.293	1.303	4.436
$2\theta_{\text{range}} [^\circ]$	2.76–26.37	3.50–26.05	2.28–25.98	2.75–25.35	3.01–27.02	2.04–25.00
measured refl.	46115	38087	38037	20650	77312	9181
independent refl.	6128	3924	9976	3622	12185	7105
Refined parameters	338	217	565	205	591	437
$R1 (I > 2\sigma I)$	0.0284	0.0708	0.0432	0.1223	0.0407	0.0971
wR2 (all data)	0.0755	0.0757	0.0625	0.0936	0.0741	0.1059
residual electron density [ $e \text{ \AA}^{-3}$ ]	0.220/–0.209	0.410/–0.397	0.312/–0.391	0.628/–0.369	0.316/–0.237	0.616/–0.575

[a] Diffractometer: Stoe, IPDS; Structure solution by direct methods, SHELXL, SIR 92; refinement: full-matrix least-squares methods against  $F^2$ .

Table 3. Selected bond lengths ( $\text{\AA}$ ) and angles ( $^\circ$ ) for complexes **4**, **8** and **7b**.

$[[\text{Cp}^*\text{Fe}][\text{Cp}^R\text{CoP}_4][\text{FeCp}^*]]$ ( <b>4</b> ), $\text{Cp}^R = \text{C}_5\text{H}_4\text{tBu}$							
Fe1–P1	2.3994(5)	Fe2–P1	2.3965(5)	P1–P2	2.1859(7)	P1–Co1–P4	98.78(2)
Fe1–P2	2.3595(6)	Fe2–P2	2.3615(5)	P2–P3	2.1353(8)	Co1–P1–P2	115.26(2)
Fe1–P3	2.3528(6)	Fe2–P3	2.3558(5)	P3–P4	2.1832(8)	P1–P2–P3	105.47(3)
Fe1–P4	2.3743(6)	Fe2–P4	2.3738(5)	Co1–P1	2.1570(5)	P2–P3–P4	104.87(3)
Fe1–Co1	2.6491(4)	Fe2–Co1	2.6440(4)	Co1–P4	2.1615(6)	P3–P4–Co1	115.63(3)
Fe1– $\text{Cp}_{(\text{cent})}^*$	1.725	Fe2– $\text{Cp}_{(\text{cent})}^*$	1.73	Co1– $\text{Cp}_{(\text{cent})}^*$	1.71	$\text{Cp}_{(\text{cent})}^*\text{-Fe1-Fe2}$	172.4
				$\text{Cp}_{(\text{cent})}^*\text{-Fe2-Fe1}$	171.9		
$[[\text{Cp}^*\text{Fe}](\mu_4\text{-}\eta^5\text{-}\eta^2\text{-}\eta^1\text{-P}_3)[\text{Co}(\text{CO})\text{Cp}^R][\text{Co}_2\text{Cp}_2^R(\mu\text{-CO})]]$ ( <b>8</b> ), $\text{Cp}^R = \text{C}_5\text{H}_3\text{tBu}_{2-1,3}$							
Fe1–P1	2.3938(5)	Co3–P3	2.1290(5)	P2–P1–P5	99.19(2)	P1–Co1–Co2	56.858(15)
Fe1–P2	2.3699(6)	Co1–Co2	2.4758(4)	P1–P2–P3	109.06(3)	Co1–P1–Co2	65.599(15)
Fe1–P3	2.4338(5)	P1–P2	2.3541(7)	P2–P3–P4	111.68(3)	P1–Co2–Co1	57.544(14)
Fe1–P4	2.3696(6)	P5–P1	2.3542(7)	P3–P4–P5	107.79(3)	P1–Co2–P2	61.879(18)
Fe1–P5	2.3606(6)	P2–P3	2.1378(6)	P1–P5–P4	111.37(3)	P1–P2–Co2	58.519(17)
Co1–P1	2.2940(5)	P3–P4	2.1306(7)	Co1–P1–P5	58.595(18)	P2–P1–Co2	59.602(18)
Co1–P5	2.2752(5)	P4–P5	2.1301(7)	P1–P5–Co1	59.380(18)		
Co2–P1	2.2764(5)	$\text{Cp}_{(\text{cent})}^*\text{-Fe}$	1.75	P1–Co1–P5	62.025(18)		
Co2–P2	2.3023(5)	Co1, 2, 3– $\text{Cp}_{(\text{cent})}^*$	1.76, 1.78, 1.72				
$[[\text{Cp}^R\text{Co}]_3(\mu_3\text{-P}_2)]$ ( <b>7b</b> ), $\text{Cp}^R = \text{C}_5\text{H}_3\text{tBu}_{2-1,3}$							
Co1(1')–P1(1)	2.1718(14)	$\text{Cp}_{(\text{cent})}^*\text{-Co1(1')}$	1.72	Co1(1')–Co2–Co1(1)	61.82(2)		
Co2–P1(1')	2.1626(15)	$\text{Cp}_{(\text{cent})}^*\text{-Co2}$	1.77	Co2–Co1(1')–Co1(1)	59.09(2)		
Co1–Co1'	2.5781(14)	Co1(1')–P1(1')	2.1576(15)	P1–Co1(1')–P1'	94.92(6)		
Co1(1')–Co2	2.5097(10)			P1(1')–Co2–P1'(1)	95.04(8)		

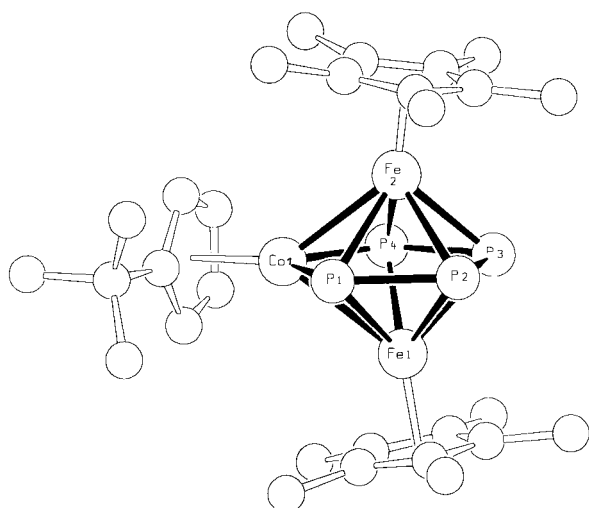


Figure 1. Structure of [[Cp\*Fe][Cp<sup>R</sup>CoP<sub>4</sub>][FeCp\*]] (**4**) in the crystal.

$[[\text{Cp}^*\text{Fe}](\mu_4\text{-}\eta^5\text{:}\eta^2\text{:}\eta^2\text{:}\eta^1\text{-P}_5)\{\text{Co}(\text{CO})\text{Cp}^R\}\{\text{Co}_2\text{Cp}_2^R(\mu\text{-CO})\}]$  (**8**; Cp<sup>R</sup> = C<sub>5</sub>H<sub>3</sub>tBu<sub>2</sub>-1,3): The most interesting part of the structure of **8** is the cyclo-P<sub>5</sub> ligand with additional double side-on binding ( $\eta^2$ ) to the Co<sub>2</sub>Cp<sub>2</sub><sup>R</sup>( $\mu$ -CO) fragment and further terminal coordination ( $\eta^1$ ) of a 16 VE Cp<sup>R</sup>(OC)Co fragment (Figure 2). As a consequence of the  $\eta^2$  coordination mode, P<sub>2</sub>–P<sub>1</sub> and P<sub>1</sub>–P<sub>5</sub> are elongated to 2.35 Å (Table 3); this is close to the value of 2.36 Å<sup>[1c]</sup> found in [[Cp\*Fe]( $\mu$ - $\eta^5\text{:}\eta^2\text{-P}_5$ )[Ir(CO)Cp\*]] (**16**).

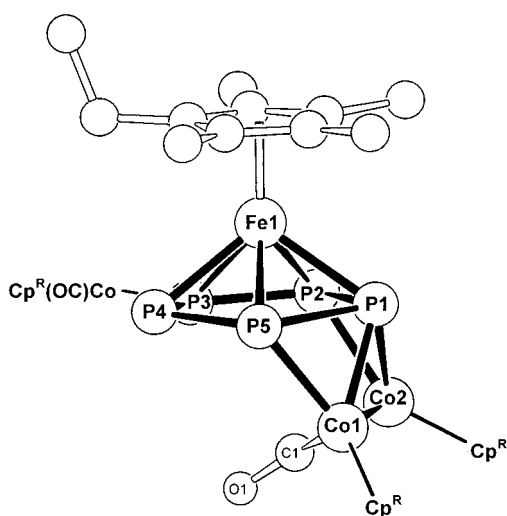


Figure 2. Structure of [[Cp\*Fe]( $\mu_4\text{-}\eta^5\text{:}\eta^2\text{:}\eta^2\text{:}\eta^1\text{-P}_5$ ){Co(CO)Cp<sup>R</sup>}{Co<sub>2</sub>Cp<sub>2</sub><sup>R</sup>( $\mu$ -CO)}] (**8**) in the crystal. Cp<sup>R</sup> = C<sub>5</sub>H<sub>3</sub>tBu<sub>2</sub>-1,3.

In sandwich complexes of the type [Cp<sup>R</sup>Fe{(CR)<sub>3</sub>P<sub>2</sub>}M<sub>2</sub>(CO)<sub>n</sub>] (**17**; Cp<sup>R</sup> = C<sub>5</sub>H<sub>3</sub>tBu<sub>2</sub>-1,3, R = OSiMe<sub>3</sub>; M = Fe,  $n = 7$ <sup>[16a]</sup>; M = Co,  $n = 6$ <sup>[16b]</sup>) the five-membered C<sub>3</sub>P<sub>2</sub> ring has one P–P bond that coordinates in an additional  $\eta^2\text{:}\eta^1$  mode to M<sub>2</sub>(CO)<sub>n</sub>. The sum of bond angles in the P<sub>5</sub> ring of **8** was found to be 539.1° (smallest angle = 99.2° at P<sub>1</sub> with a formal connectivity of five; Figure 2). It is worthwhile to note the difference in the P–P and Fe–P bond lengths (Table 3). In **8**  $\bar{d}(\text{P–P})$  is 2.13 Å for the bonds that have no further  $\eta^2$ -

coordination (c.f. 2.12 Å in compound **16**<sup>[1c]</sup>). Interestingly, the longest Fe1–P<sub>3</sub> bond length of 2.43 Å involves the P atom with an additional terminally coordinated Co(CO)Cp<sup>R</sup> fragment (Figure 2). The smallest distance belongs to the Fe1–P<sub>5</sub> bond (2.36 Å). The Co–P bond lengths of the side-on binding Co<sub>2</sub>Cp<sub>2</sub><sup>R</sup>( $\mu$ -CO) moiety are between 2.275 and 2.30 Å, whereas Co<sub>3</sub>–P<sub>3</sub> with a classical coordination to a P lone-pair of the cyclo-P<sub>5</sub> ring is distinctly shorter (2.13 Å). With 2.48 Å, the Co1–Co<sub>2</sub> bond length is in the typical range of a single bond. Compared with **16**, in which the dihedral angle of the FeP<sub>2</sub>Ir butterfly structural subunit is 158.5°<sup>[1c]</sup>, the Fe1, P<sub>1</sub>, P<sub>5</sub>, Co1 and Fe1, P<sub>1</sub>, P<sub>2</sub>, Co<sub>2</sub> subunits of **8** show folding angles of 151° and 153.8°, respectively. The angle Fe1–P<sub>1</sub>–Co1(2), for the midpoint between Co1 and Co2, was found to be 118.3°.

The geometry of the eight-atom FeCo<sub>2</sub>P<sub>5</sub> skeleton can formally be derived from an icosahedron with four missing vertices (Figure 3a). On the other hand, the electron count

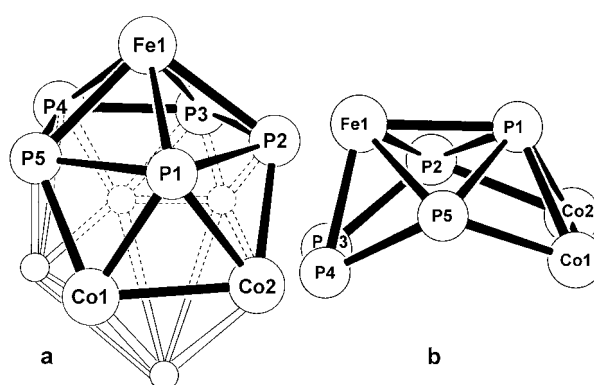
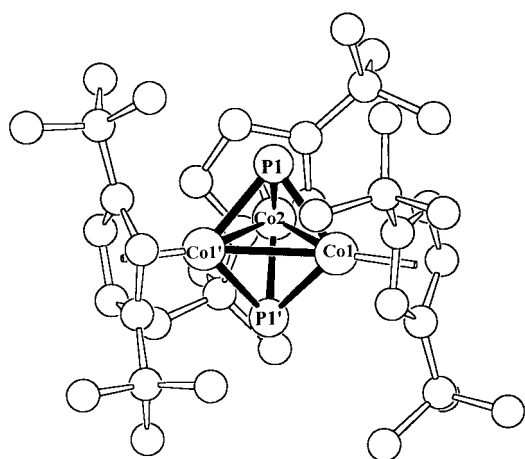


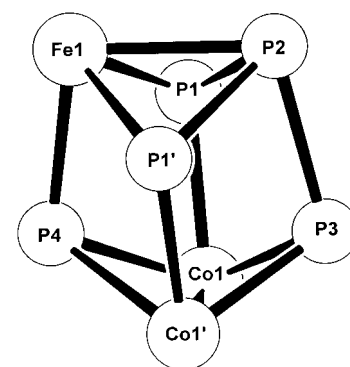
Figure 3. a) FeCo<sub>2</sub>P<sub>5</sub> skeleton formally derived from an icosahedron. b) FeCo<sub>2</sub>P<sub>5</sub> skeleton described as two penetrating five-membered rings (FeP<sub>2</sub>Co<sub>2</sub>/P<sub>5</sub>) capped by P<sub>1</sub> and Fe1, respectively.

according to the Wade–Mingos rules<sup>[14]</sup> gives 11 SEPs, which is in accordance with a ( $n+3$ ) arachno-type structure derived from a bicapped square antiprism in which two corners have been eliminated (c.f. B<sub>8</sub>H<sub>14</sub>, a B<sub>n</sub>H<sub>n+6</sub> arachno borane<sup>[17]</sup>). Another structural description is based on two penetrating five-membered rings (P<sub>5</sub> and Co<sub>2</sub>P<sub>2</sub>Fe) capped by Fe1 and P<sub>1</sub>, respectively (Figure 3b).

$[[\text{Cp}^R\text{Co}]_3(\mu_3\text{-P})_2]$  (**7b**; Cp<sup>R</sup> = C<sub>5</sub>H<sub>3</sub>tBu<sub>2</sub>-1,3): Compound **7b** (Figure 4) was synthesized for the first time by T. Mohr<sup>[18]</sup> by cothermolysing [[Cp\*Fe][Cp<sup>R</sup>TaP<sub>5</sub>]]<sup>[4]</sup> and [Cp<sup>R</sup>Co(CO)<sub>2</sub>]. The Co–Co distances of **7b** lie between 2.51 and 2.58 Å (isosceles triangle). The trigonal bipyramidal Co<sub>3</sub>P<sub>2</sub> skeleton forms nearly equal P–Co–P bond angles (94.9 to 95.0°). The same holds for the Co–P distances. Both can be compared with the ( $\mu_3\text{-P}$ )Co<sub>3</sub>Cp<sub>3</sub><sup>R</sup> fragment of [( $\mu_3\text{-P}$ ){Co<sub>3</sub>Cp<sub>3</sub><sup>R</sup>}( $\mu_3\text{-PSe}$ )] (**18**), the first complex with a  $\mu_3\text{-PSe}$  ligand.<sup>[11]</sup> To the best of our knowledge, **7b** is the only example of a [L<sub>n</sub>M]<sub>3</sub>( $\mu_3\text{-P}$ )<sub>2</sub>] cluster (L<sub>n</sub>M means 14 VE fragment) that has been synthesized and structurally characterized (c.f. compound **14**<sup>[12]</sup> with ML<sub>n</sub> as Fe(CO)<sub>4</sub> and additional coordination of one P atom to a Mn(CO)<sub>2</sub>Cp fragment). The electron count<sup>[14]</sup> for **7b** (6 SEPs) is in accordance with a typical closo ( $n+1$ ) cluster.

Figure 4. Structure of  $[[\text{Cp}^{\text{R}}\text{Co}]_3(\mu_3\text{-P})_2]$  (**7b**) in the crystal.

$[[\text{Cp}^{\text{R}}\text{Fe}][\text{Cp}^{\text{R}}\text{Co}]_2(\text{P}_4)(\text{P})]$  (**5**;  $\text{Cp}^{\text{R}} = \text{C}_5\text{H}_3\text{tBu}_{2-1,3}$ ): Comparing the mean P–P distance of 2.27 Å for the tripodal  $\text{P}_4$  ligand in **5** with that of  $[[\text{Cp}^{\text{R}}\text{Ni}]_3(\text{P}_4)(\text{P})]$  (**19**)<sup>[19]</sup> (2.21 Å as in white phosphorus itself) an elongation can be observed. For the more symmetric compound **19** the P–P–P bond angles of the pyramidal  $\text{P}_4$  ligand lie within the narrow range of 83.0–84.3°<sup>[19]</sup>, whereas a much greater difference (72.9–94.4°) was found for the heterometallic complex **5**. Of special interest are the bond lengths of the diagonally arranged atoms in the quadrangles of the distorted cubanelike  $\text{FeCo}_2\text{P}_5$  skeleton (Figure 5).  $\text{P3}\cdots\text{P4} = 3.17$ ,  $\text{P1}\cdots\text{P1}' = 3.30$ ,  $\text{P1}(1')\cdots\text{P3} = 2.70$ ,  $\text{P1}(1')\cdots\text{P4} = 2.56$ ,  $\text{Fe1}\cdots\text{Co1}(1') = 3.64$ , and  $\text{P2}\cdots\text{Co1}(1') = 3.56$  Å are nonbonding, while  $\text{Fe1}-\text{P2}$  (2.36 Å) and  $\text{Co1}-\text{Co1}'$  (2.56 Å) are in the bonding range (c.f. complexes **7b** and **8**, Table 3; **6b**, Table 4). Complex **5** shows an interesting parallel to  $[[\text{CpCo}]_4\text{P}_4]$  (**20**) synthesized and characterized by X-ray crystallography for the first time in 1973 by Dahl et al.<sup>[20]</sup> (see also X-ray crystal structure discussion of **6b**). As described for **20**, the most severe

Figure 5. Skeleton structure of  $[[\text{Cp}^{\text{R}}\text{Fe}][\text{Cp}^{\text{R}}\text{Co}]_2(\text{P}_4)(\text{P})]$  (**5**) in the crystal.  $\text{Cp}^{\text{R}}$  and  $\text{Cp}^{\text{R}}$  ligands ( $\text{Cp}^{\text{R}} = \text{C}_5\text{H}_3\text{tBu}_{2-1,3}$ ) have been omitted for clarity.

deviation from a cubanelike structure in **5** results from the two butterfly like halves  $\text{P1}, \text{P2}, \text{Fe1}, \text{P1}'$  (dihedral angle = 120.7°) and  $\text{P3}, \text{Co1}, \text{Co1}', \text{P4}$  (120°), which are connected by the wing-tip atoms  $\text{P1}$  and  $\text{P1}'$  and the hinge atoms  $\text{Co1}$  and  $\text{Co1}'$  as shown in Figure 5. Small differences are found for  $\text{P1}-\text{Fe1}-\text{P1}'$  (96.0°) and  $\text{P1}-\text{P2}-\text{P1}'$  (94.4°) compared with  $\text{P3}-\text{Co1}(1')-\text{P4}$  (90.4°). The strong distortion from a cubanelike  $\text{FeCo}_2\text{P}_5$  skeleton can also be seen from the following bond angles in complex **5**:  $\text{Fe1}-\text{P4}-\text{Co1}(1') = 107.5^\circ$ ,  $\text{P2}-\text{P3}-\text{Co1}(1')$  and  $\text{P2}-\text{P1}(1')-\text{Co1}(1') = 104.6^\circ$ ,  $\text{Fe1}-\text{P1}(1')-\text{Co1}(1') = 109.2^\circ$ . The deviations from the least-squares mean planes are as follows:  $\text{Fe1}, \text{P4}, \text{P1}(1'), \text{Co1}(1') = 0.15$  Å;  $\text{Co1}(1'), \text{P1}(1'), \text{P2}, \text{P3} = 0.12$  Å;  $\text{P3}, \text{Co1}, \text{P4}, \text{Co1}' = 0.46$  Å;  $\text{Fe1}, \text{P1}, \text{P2}, \text{P1}' = 0.47$  Å.

$[[\text{Cp}^{\text{R}}\text{Co}]_4\text{P}_4]$  (**6b**;  $\text{Cp}^{\text{R}} = \text{C}_5\text{H}_3\text{tBu}_{2-1,3}$ ): The comparison of **6b** with the Cp analogue  $[[\text{CpCo}]_4\text{P}_4]$  (**20**)<sup>[20]</sup> shows an interesting influence of the Cp substituents with respect to the structure of the  $\text{Co}_4\text{P}_4$  skeleton (Figure 6). Whereas the  $\text{FeCo}_2\text{P}_5$  skeleton of complex **5** (Figure 5) shows a remarkable parallel to the  $\text{Co}_4\text{P}_4$  core of compound **20**<sup>[20]</sup> (Figure 6), the

Table 4. Selected bond lengths (Å) and angles (°) for complexes **5** and **6b**.

$[[\text{Cp}^{\text{R}}\text{Fe}][\text{Cp}^{\text{R}}\text{Co}]_2(\text{P}_4)(\text{P})]$ ( <b>5</b> ), $\text{Cp}^{\text{R}} = \text{C}_5\text{H}_3\text{tBu}_{2-1,3}$			
$\text{Fe1}-\text{P1}(1')$	2.2221(9)	$\text{P1}(1')-\text{P2}$	2.2506(13)
$\text{Fe1}-\text{P2}$	2.3556(13)	$\text{P2}-\text{P3}$	2.2987(18)
$\text{Fe1}-\text{P4}$	2.2483(15)	$\text{P3}-\text{Co1}(1')$	2.1971(10)
$\text{Co1}(1')-\text{P1}(1')$	2.2445(10)		
$\text{Co1}(1')-\text{P4}$	2.2666(9)	$\text{P1}(1')\cdots\text{P4}$	2.5576(13)
$\text{Co1}-\text{Co1}'$	2.5580(8)	$\text{P1}(1')\cdots\text{P3}$	2.70
$\text{Fe1}-\text{Cp}^{\text{R}}_{(\text{cent})}$	1.75	$\text{P3}\cdots\text{P4}$	3.17
$\text{Co1}-\text{Cp}^{\text{R}}_{(\text{cent})}$	1.75	$\text{P1}\cdots\text{P1}'$	3.30
$\text{Fe1}\cdots\text{Co1}(1')$	3.64	$\text{P2}\cdots\text{Co1}(1')$	3.56
$[[\text{Cp}^{\text{R}}\text{Co}]_4\text{P}_4]$ ( <b>6b</b> ), $\text{Cp}^{\text{R}} = \text{C}_5\text{H}_3\text{tBu}_{2-1,3}$			
$\text{Co1}-\text{Co2}$	2.5246(4)	$\text{Co3}-\text{P1}$	2.2621(7)
$\text{Co3}-\text{Co4}$	2.5176(4)	$\text{Co3}-\text{P2}$	2.2054(7)
$\text{Co1}\cdots\text{Co4}$	3.60	$\text{Co3}-\text{P3}$	2.2794(6)
$\text{Co2}\cdots\text{Co3}$	3.60	$\text{Co4}-\text{P1}$	2.2056(6)
$\text{Co1}-\text{P1}$	2.2759(7)	$\text{Co4}-\text{P2}$	2.2574(7)
$\text{Co1}-\text{P3}$	2.2675(7)	$\text{Co4}-\text{P4}$	2.2827(7)
$\text{Co1}-\text{P4}$	2.2081(5)	$\text{P1}-\text{P3}$	2.3882(8)
$\text{Co2}-\text{P2}$	2.2769(6)	$\text{P2}-\text{P4}$	2.3908(8)
$\text{Co2}-\text{P3}$	2.2051(7)	$\text{P2}\cdots\text{P3}$	2.6782(7)
$\text{Co2}-\text{P4}$	2.2687(7)	$\text{P1}\cdots\text{P4}$	2.6758(8)
		$\text{Cp}^{\text{R}}_{(\text{cent})}-\text{Co1,2,3,4}$	1.77, 1.77, 1.77, 1.765
		$\text{P3}-\text{Co1}-\text{P1}$	63.42(2)
		$\text{P1}-\text{Co1}-\text{P4}$	73.26(2)
		$\text{P3}-\text{Co1}-\text{P4}$	88.53(2)
		$\text{P2}-\text{Co2}-\text{P4}$	63.47(2)
		$\text{P2}-\text{Co2}-\text{P3}$	73.37(2)
		$\text{P3}-\text{Co2}-\text{P4}$	88.58(2)
		$\text{P1}-\text{Co3}-\text{P3}$	63.45(2)
		$\text{P2}-\text{Co3}-\text{P3}$	73.32(2)
		$\text{P1}-\text{Co3}-\text{P2}$	88.27(2)
		$\text{P2}-\text{Co4}-\text{P4}$	63.55(2)
		$\text{P1}-\text{Co4}-\text{P4}$	73.17(2)
		$\text{P1}-\text{Co4}-\text{P2}$	88.39(2)
		$\text{P1}(1')-\text{P2}-\text{P3}$	72.93(4)
		$\text{Co1}(1')-\text{P1}(1')-\text{P2}$	104.59(5)
		$\text{Fe1}-\text{P1}(1')-\text{P2}$	63.56(4)
		$\text{P1}-\text{P2}-\text{P1}'$	94.43(7)
		$\text{P1}-\text{Fe1}-\text{P1}'$	96.03(5)
		$\text{Co3}-\text{P1}-\text{Co4}$	68.58(2)
		$\text{Co1}-\text{P1}-\text{Co4}$	106.91(3)
		$\text{Co1}-\text{P1}-\text{Co3}$	113.00(3)
		$\text{Co3}-\text{P2}-\text{Co4}$	68.67(2)
		$\text{Co2}-\text{P2}-\text{Co3}$	106.67(2)
		$\text{Co2}-\text{P2}-\text{Co4}$	113.04(3)
		$\text{Co1}-\text{P3}-\text{Co2}$	68.71(2)
		$\text{Co2}-\text{P3}-\text{Co3}$	106.60(2)
		$\text{Co1}-\text{P3}-\text{Co3}$	112.66(3)
		$\text{Co1}-\text{P4}-\text{Co2}$	68.64(2)
		$\text{Co1}-\text{P4}-\text{Co4}$	106.60(3)
		$\text{Co2}-\text{P4}-\text{Co4}$	112.39(3)

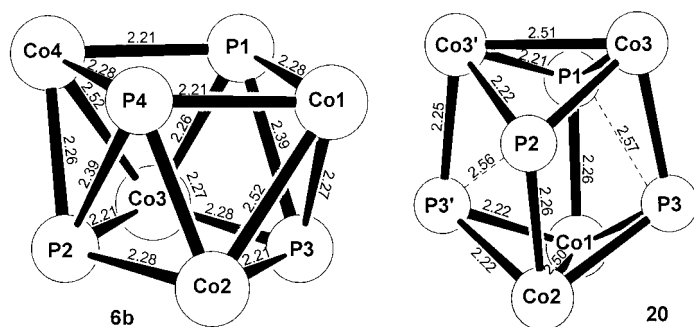


Figure 6. Comparison of bond lengths and structural differences for the skeletons of  $[[\text{Cp}^R\text{Co}]_4\text{P}_4]$  (**6b**,  $\text{Cp}^R = \text{C}_5\text{H}_3\text{tBu}_2\text{-1,3}$ ) and  $[[\text{CpCo}]_4\text{P}_4]$  (**20**,  $\text{Cp} = \text{C}_5\text{H}_5$ ).

$\text{Cp}^R$  analogue **6b** differs distinctly from **20**. For example, in **6b** the P–P bond lengths of 2.39 Å are much shorter than 2.56/2.57 Å in **20** (Table 4, Figure 6). As consequence, the Co<sub>4</sub>P<sub>4</sub> skeleton of **6b** can be described as a tetragonal antiprismatic structure. Compared with **5** and **20** the deviations from the least-squares mean planes are much smaller for **6b**: Co1, P1, Co4, P4 = 0.02 Å; P3, Co3, P2, Co2 = 0.02 Å (**20**:<sup>[20]</sup> P2, Co3', P3', Co2 = 0.11 Å; Co3, P3, Co1, P1 = 0.11 Å). An average P–P bond length of 2.31 Å was found for  $[[\text{CpFe}]_4(\text{P}_2)_2]$  (**21**), a cluster with a triangulated dodecahedral Fe<sub>4</sub>P<sub>4</sub> skeleton.<sup>[21]</sup>

$[[\text{Cp}^R\text{Co}]_4(\text{P})(\text{PSe})_3]$  (**10**;  $\text{Cp}^R = \text{C}_5\text{H}_4\text{tBu}$ ): Going from the unoxidized C<sub>5</sub>H<sub>3</sub>tBu<sub>2</sub> derivative **6b** to the threefold selenated complex **10** with C<sub>5</sub>H<sub>4</sub>tBu ligands on the Co atoms, the selected mean bond lengths show the following trends (Tables 4 and 5, Figures 6 and 7). Selected mean bond lengths for compounds **6b** [**10**]: Co–Co = 2.52 Å [2.57 Å], Co–P = 2.25 Å [2.23 Å], and P–P = 2.39 Å, P⋯P = 2.68 Å [2.52/2.77 Å]. The most significant change occurs with the P–P bonds. Whereas 2.39 Å in **6b** is in the range of P–P bonds, P2⋯P4 = 2.48 Å and P1⋯P3 = 2.57 Å in **10** are on the borderline. For  $[\text{Cl}(\text{Ph}_3\text{P})_2\text{Rh}(\eta^2\text{-P}_4)]$  a P–P distance of 2.46 Å was found for the η<sup>2</sup>-coordinated edge of the intact P<sub>4</sub> tetrahedron.<sup>[22]</sup> In **10** the deviation from the least-squares mean plane for the atoms P2, Co2, P3, Co3 is 0.02 Å, which is identical with the value found for **6b**. The corresponding value for the planes P1(Se1), Co1, P4, Co4 is 0.06 Å in **10** compared with 0.02 Å in **6b**. The P–Se bond mean value of 2.12 Å for

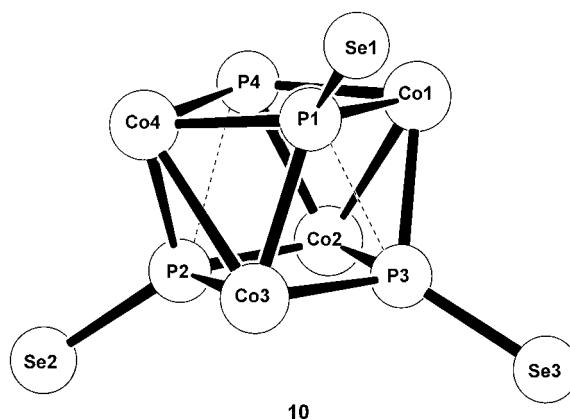


Figure 7. Skeleton structure of  $[[\text{Cp}^R\text{Co}]_4(\text{P})(\text{PSe})_3]$  (**10**);  $\text{Cp}^R(\text{C}_5\text{H}_4\text{tBu})$  ligands have been omitted for clarity.

compound **10** is slightly longer than 2.09 Å found in  $[(\mu_3\text{-P})\{\text{Cp}_3^R\text{Co}_3\}(\mu_3\text{-PSe})]$  (**18**,  $\text{Cp}^R = \text{C}_5\text{H}_3\text{tBu}_2\text{-1,3}$ )<sup>[11]</sup> and 2.10 Å in  $[[\text{CpFe}]_4(\text{P}_2\text{Se}_2)_2]$ , with two planar Se=P–P=Se ligands.<sup>[21]</sup>

For  $[[\text{Cp}^R\text{Co}]_4(\mu_3\text{-PS})_4]$  (**11**) (Scheme 2) an X-ray study has been carried out which unambiguously shows its highly symmetric structure. Due to low quality of the data set no structural details will be given. The P⋯P distances (ca. 2.70 Å) are nonbonding. The average of P=S (ca. 1.96 Å) bond lengths is in the normal range.<sup>[9]</sup>

## Experimental Section

All experiments were carried out under an argon atmosphere in dry solvents.  $[\text{Cp}^*\text{Fe}(\eta^5\text{-P}_5)]$  (**1**)<sup>[10]</sup>,  $[\text{Cp}^*\text{Fe}(\eta^5\text{-P}_5)]$  (**1'**)<sup>[10]</sup>,  $[\text{Cp}^R\text{Co}(\text{CO})_2]$  (**2a,b**)<sup>[23]</sup> and  $[[\text{Cp}^R\text{Co}(\mu\text{-CO})_2]$  (**3**)<sup>[24]</sup> were synthesized according to the literature (**1'** in analogy to the Cp\* derivatives, **2a,b** in analogy to the Cp derivatives). IR spectra were recorded on a Perkin–Elmer 881. UV-irradiation: 150 W high-pressure lamp, TQ 150, Heraeus Quarzlampen GmbH, Hanau.

**Reaction of  $[\text{Cp}^*\text{FeP}_5]$  (**1**) with  $[\text{Cp}^R\text{Co}(\text{CO})_2]$  (**2a**) to give **4**, **6a**, and **7a**:** Compound **1** (440 mg, 1.27 mmol) and **2a** (500 mg, 2.12 mmol) were dissolved in decalin (ca. 50 mL), and the mixture was stirred and heated to reflux for about 2 h until the ν(CO) band in the IR spectra of **2a** disappeared. After evaporation of the solvent under oil-pump vacuum, the residue was dissolved in dichloromethane (ca. 8 mL; small amounts of  $[[\text{Cp}^*\text{Fe}]_2(\text{P}_2)_2]$  could be detected by <sup>31</sup>P-NMR spectroscopy), neutral Al<sub>2</sub>O<sub>3</sub> (ca. 2 g, activity grade II) was added, and the mixture was concentrated until it was flowed freely. Column chromatography (column

Table 5. Selected bond lengths (Å) and angles (°) for complex **10**.

$[[\text{Cp}^R\text{Co}]_4(\text{P})(\text{PSe})_3]$ ( <b>10</b> ), $\text{Cp}^R = \text{C}_5\text{H}_4\text{tBu}$							
Co1–Co2	2.5508(12)	Co4–P1	2.1671(17)	P1–Co1–P3	70.67(7)	Co1–P1–Co3	106.34(7)
Co3–Co4	2.5836(12)	Co4–P2	2.2127(19)	P1–Co1–P4	76.13(6)	Co3–P2–Co4	71.35(6)
Co1⋯Co4	3.50	Co4–P4	2.2976(18)	P3–Co1–P4	93.94(7)	Co2–P2–Co3	101.34(7)
Co2⋯Co3	3.45	P1⋯P3	2.559(2)	P2–Co2–P4	66.97(6)	Co2–P2–Co4	110.97(8)
Co1–P1	2.2120(19)	P2⋯P3	2.80	P2–Co2–P3	78.05(6)	Co1–P3–Co2	70.54(6)
Co1–P3	2.2130(19)	P2⋯P4	2.478(2)	P3–Co2–P4	93.74(7)	Co2–P3–Co3	102.33(7)
Co1–P4	2.2368(17)	P1⋯P4	2.74	P1–Co3–P3	69.67(6)	Co1–P3–Co3	107.64(7)
Co2–P3	2.2047(18)	P1–Se1	2.1233(18)	P2–Co3–P3	78.17(6)	Co1–P4–Co2	69.25(5)
Co2–P2	2.2392(18)	P2–Se2	2.1218(17)	P1–Co3–P2	89.79(7)	Co1–P4–Co4	101.21(7)
Co2–P4	2.2522(19)	P3–Se3	2.1257(17)	P2–Co4–P4	66.63(7)	Co2–P4–Co4	107.46(8)
Co3–P2	2.2176(18)	$\text{Cp}^R_{(\text{cent})}\text{-Co1, 2, 3, 4}$	1.74, 1.75, 1.74, 1.74	P1–Co4–P4	75.75(6)	Co–P–Se	117.4–125.7
Co3–P1	2.259(2)			P1–Co4–P2	92.34(7)	P–P–Se	129.8–132.0
Co3–P3	2.2210(17)			Co3–P1–Co4	71.39(6)		
				Co1–P1–Co4	106.30(8)		

12 × 1.5 cm, neutral Al<sub>2</sub>O<sub>3</sub>(II), petroleum ether) with petroleum ether afforded a red-violet fraction 20 mg (5% yield) of [[Cp<sup>R</sup>Co]<sub>3</sub>(μ<sub>3</sub>-P)<sub>2</sub>] (**7a**). With petroleum ether/toluene (30:1) 300 mg (67% yield) of green [[Cp<sup>R</sup>Co]<sub>4</sub>P<sub>4</sub>] (**6a**) was eluted. A 10:1 mixture gave 150 mg (10% yield) of **4** as a dark brown fraction. **4**: C<sub>29</sub>H<sub>43</sub>CoFe<sub>2</sub>P<sub>4</sub> (686.1): calcd C 50.76, H 6.32; found C 49.97, H 6.15. **6a**: C<sub>36</sub>H<sub>52</sub>Co<sub>4</sub>P<sub>4</sub> (844.4): calcd C 51.21, H 6.21; found C 51.79, H 6.10. **7a**: C<sub>27</sub>H<sub>39</sub>Co<sub>3</sub>P<sub>2</sub> (602.3): calcd C 53.84, H 6.53; found C 53.05, H 6.61.

**Reaction of 1 with 2b to form of 5, 6b, and 7b**: Compound **1** (294 mg, 0.85 mmol) and **2b** (740 mg, 2.53 mmol) were dissolved in decalin (ca. 110 mL), and the mixture was stirred and heated to reflux for about 100 min [IR control and column chromatography (basic Al<sub>2</sub>O<sub>3</sub>(II), column 15 × 2.0 cm) as described above]. Traces of [[Cp<sup>R</sup>Fe]<sub>2</sub>(P<sub>2</sub>)<sub>2</sub>]<sup>[7]</sup> and [[Cp<sup>R</sup>Co]<sub>2</sub>(P<sub>2</sub>)<sub>2</sub>]<sup>[8]</sup> were detected by <sup>31</sup>P NMR spectroscopy. Petroleum ether as eluent gave 50 mg (8% yield) of **7b** as a red-violet fraction. 290 mg (43% yield) of green **6b** were eluted with a 50:1 mixture of petroleum ether/toluene, and 120 mg (12% yield) of brown **5** were isolated from a 10:1 mixture. **5**: C<sub>36</sub>H<sub>57</sub>FeCo<sub>2</sub>P<sub>5</sub> (818.4): calcd C 52.83, H 7.02; found C 52.60, H 7.04. **6b**: C<sub>52</sub>H<sub>84</sub>Co<sub>4</sub>P<sub>4</sub> (1068.8): calcd C 58.43, H 7.92; found C 58.67, H 7.82. **7b**: C<sub>39</sub>H<sub>65</sub>Co<sub>3</sub>P<sub>2</sub> (770.6): calcd C 60.78, H 8.24; found C 60.30, H 8.15.

**Photochemical reaction of [(C<sub>2</sub>Me<sub>4</sub>Et)FeP<sub>2</sub>] (**1'**) with [[Cp<sup>R</sup>Co(μ-CO)]<sub>2</sub>] (**3**) to give **8****: Compound **1'** (360 mg, 1 mmol) and **3** (529 mg, 1 mmol), each dissolved in a small volume of toluene, were placed in a UV apparatus containing toluene (100 mL). The water-cooled mixture was irradiated for about 390 min until the CO band in the IR spectrum of **3** disappeared. After evaporation of the solvent, the black oily residue was dissolved in petroleum ether (ca. 7 mL) and chromatographed (column 10 × 2.0 cm, neutral Al<sub>2</sub>O<sub>3</sub>(II), petroleum ether). With petroleum ether traces of [Cp<sup>R</sup>Co(CO)]<sub>2</sub> (**2b**) were detected. Further elution with the same solvent gave a blue fraction (oily, no <sup>31</sup>P NMR signal) and after that a brown-violet fraction containing 390 mg (53% yield) of **8**. C<sub>52</sub>H<sub>60</sub>Co<sub>3</sub>FeO<sub>2</sub>P<sub>5</sub> (1124.65): calcd C 55.53, H 7.17; found C 55.08, H 7.14; IR (toluene):  $\tilde{\nu}(\text{CO}) = 1927(\text{s}), 1791(\text{brs}, \mu\text{-CO})$ .

**Oxidation of [[Cp<sup>R</sup>Co]<sub>4</sub>P<sub>4</sub>] (**6a** and **6b**) with S<sub>8</sub> to the sulfurized products **9** and **12****: Compound **6a** (480 mg, 0.57 mmol) [**6b** (110 mg, 0.103 mmol)] and S<sub>8</sub> (146 mg, 0.57 mmol) [53 mg, 0.207 mmol] were dissolved in toluene (30 mL) [10 mL] and stirred for 48 h at room temperature. After evaporation of the solvent, the brown residue was dissolved in dichloromethane (ca. 5 mL). Silica gel (ca. 1.5 g, II) was added and the mixture was concentrated until it flowed freely. Chromatography (column 10 × 1.0 cm, silica gel (II), petroleum ether) with a mixture of petroleum ether/toluene (20:1) gave green-brown fractions of 390 mg (73% yield) [[Cp<sup>R</sup>Co]<sub>4</sub>(PS)<sub>3</sub>(P)] (**9**) [75 mg (64% yield) **12**]. **9**: C<sub>36</sub>H<sub>52</sub>Co<sub>4</sub>P<sub>4</sub>S<sub>3</sub> (940.6): calcd C 45.97, H 5.57; found C 45.84, H 5.57. **12**: C<sub>52</sub>H<sub>84</sub>Co<sub>4</sub>P<sub>4</sub>S<sub>2</sub> (1132.9): calcd C 55.13, H 7.47; found C 54.86, H 7.43.

**Oxidation of 6a and 6b with grey selenium to give [[Cp<sup>R</sup>Co]<sub>4</sub>(PSe)<sub>3</sub>(P)] (**10**) and [[Cp<sup>R</sup>Co]<sub>4</sub>(PSe)<sub>2</sub>P<sub>2</sub>] (**13**)**: Compound **6a** (400 mg, 0.474 mmol) [**6b** (80 mg, 0.075 mmol)] and grey selenium (300 mg, 3.80 mmol) [50 mg, 0.63 mmol] were stirred for 24 h in dichloromethane (20 mL) (<sup>31</sup>P NMR control). Workup as described for **9** and **12**. Neutral Al<sub>2</sub>O<sub>3</sub>(II) was used instead of silica gel. With petroleum ether/toluene (1:1) green-brown fractions of **10** and **13** were eluted. **10**: 240 mg (47% yield); C<sub>36</sub>H<sub>52</sub>Co<sub>4</sub>P<sub>4</sub>Se<sub>3</sub> (1081.3): calcd C 39.99, H 4.85; found C 39.97, H 4.78. **13**: 25 mg (27% yield); C<sub>52</sub>H<sub>84</sub>Co<sub>4</sub>P<sub>4</sub>Se<sub>2</sub> (1226.7) calcd C 50.91, H 6.90; found C 49.98, H 7.04.

**Oxidation of 9 to [[Cp<sup>R</sup>Co]<sub>4</sub>(μ<sub>3</sub>-PS)<sub>4</sub>] (**11**)**: Compound **9** (180 mg, 0.19 mmol) and S<sub>8</sub> (13 mg, 0.05 mmol) were heated to reflux in dichloromethane (25 mL) for 24 h. Workup as described before for **9** and **12** (silica gel(II)). A mixture of petroleum ether/toluene (5:1) gave 120 mg (63% yield) of **11** as a brown fraction. C<sub>36</sub>H<sub>52</sub>Co<sub>4</sub>P<sub>4</sub>S<sub>4</sub> (972.7): calcd C 44.45, H 5.34; found C 44.26, H 5.18.

**Single-crystal X-ray structure determinations**: See also Table 2. Crystallographic data (excluding structure factors) for the structures reported in this paper have been deposited with the Cambridge Crystallographic Data Centre as supplementary publication nos. CCDC-101528, CCDC-101529, CCDC-101530, CCDC-101531, CCDC-101532, and CCDC-101533. Copies of the data can be obtained free of charge on application to CCDC, 12 Union Road, Cambridge CB2 1EZ (fax: (+44)1223-336-033; e-mail: deposit@ccdc.cam.ac.uk).

**Acknowledgments**: We thank the DFG (stipend to S.W.), the Fonds der Chemischen Industrie, and the Graduiertenkolleg: Phosphorus Chemistry as a Link between Different Chemical Disciplines for financial support.

Received: April 1, 1998 [F1080]

- [1] a) O. J. Scherer, T. Brück, *Angew. Chem.* **1987**, *99*, 59; *Angew. Chem. Int. Ed. Engl.* **1987**, *26*, 59; b) O. J. Scherer, T. Brück, G. Wolmershäuser, *Chem. Ber.* **1988**, *121*, 935; c) improved synthesis: M. Detzel, G. Friedrich, O. J. Scherer, G. Wolmershäuser, *Angew. Chem.* **1995**, *107*, 1454; *Angew. Chem. Int. Ed. Engl.* **1995**, *34*, 1321; d) M. Baudler, S. Akpapoglou, D. Ouzounis, F. Wasgestian, B. Meinigke, H. Budzickiewicz, H. Münster, *Angew. Chem.* **1988**, *100*, 288; *Angew. Chem. Int. Ed. Engl.* **1988**, *27*, 280.
- [2] Recent reviews: a) O. J. Scherer, *Angew. Chem.* **1990**, *102*, 1137; *Angew. Chem. Int. Ed. Engl.* **1990**, *29*, 1104; b) M. Scheer, E. Herrmann, *Z. Chem.* **1990**, *30*, 41.
- [3] O. J. Scherer, T. Brück, G. Wolmershäuser, *Chem. Ber.* **1989**, *122*, 2049.
- [4] M. Detzel, T. Mohr, O. J. Scherer, G. Wolmershäuser, *Angew. Chem.* **1994**, *106*, 1142; *Angew. Chem. Int. Ed. Engl.* **1994**, *33*, 1110.
- [5] O. J. Scherer, T. Mohr, G. Wolmershäuser, *J. Organomet. Chem.* **1997**, *529*, 379.
- [6] C. Hofmann, O. J. Scherer, G. Wolmershäuser, *J. Organomet. Chem.* **1998**, *559*, 219.
- [7] M. E. Barr, L. F. Dahl, *Organometallics* **1991**, *10*, 3991.
- [8] M. Scheer, U. Becker, M. H. Chisholm, J. C. Huffman, F. Lemoigno, O. Eisenstein, *Inorg. Chem.* **1995**, *34*, 3117.
- [9] a) O. J. Scherer, J. Braun, P. Walthier, G. Heckmann, G. Wolmershäuser, *Angew. Chem.* **1991**, *103*, 861; *Angew. Chem. Int. Ed. Engl.* **1991**, *30*, 852; b) J. Foerstner, F. Olbrich, H. Butenschön, *Angew. Chem.* **1996**, *108*, 1323; *Angew. Chem. Int. Ed. Engl.* **1996**, *35*, 1234; c) W. Wang, A. J. Carty, *New J. Chem.* **1997**, *21*, 773; d) J. E. Davies, M. C. Klunduk, M. J. Mays, P. R. Raithby, G. P. Shields, P. K. Tompkin, *J. Chem. Soc. Dalton Trans.* **1997**, 715; e) M. J. A. Johnson, A. L. Odom, C. C. Cummins, *Chem. Commun.* **1997**, 1523.
- [10] a) I.-P. Lorenz, W. Pohl, K. Polborn, *Chem. Ber.* **1996**, *129*, 11; b) O. J. Scherer, C. Vondung, G. Wolmershäuser, *Angew. Chem.* **1997**, *109*, 1360; *Angew. Chem. Int. Ed. Engl.* **1997**, *36*, 1303; c) J. E. Davies, M. J. Mays, E. J. Pook, P. R. Raithby, P. K. Tompkin, *Chem. Commun.* **1997**, 1997; d) C. E. Laplaza, W. M. Davis, C. C. Cummins, *Angew. Chem.* **1995**, *107*, 2181; *Angew. Chem. Int. Ed. Engl.* **1995**, *34*, 2042.
- [11] S. Weigel, G. Wolmershäuser, O. J. Scherer, *Z. Anorg. Allg. Chem.* **1998**, *624*, 559.
- [12] H. Lang, G. Huttner, L. Zsolnai, G. Mohr, B. Sigwarth, U. Weber, O. Orama, I. Jibril, *J. Organomet. Chem.* **1986**, *304*, 157; see also: B. E. Collins, Y. Koide, C. K. Schauer, P. S. White, *Inorg. Chem.* **1997**, *36*, 6172, and references therein.
- [13] X.-B. Ma, M. Birkel, T. Wettling, M. Regitz, *Heteroatom Chemistry* **1995**, *6*, 1.
- [14] K. Wade, *Adv. Inorg. Chem. Radiochem.* **1976**, *18*, 1; D. M. P. Mingos, R. L. Johnston, *Struct. Bond.* **1987**, *68*, 29.
- [15] W. Tremel, R. Hoffmann, M. Kertesz, *J. Am. Chem. Soc.* **1989**, *111*, 2030; E. D. Jemmis, A. C. Reddy, *Organometallics* **1988**, *7*, 1561.
- [16] a) L. Weber, O. Sommer, H.-G. Stämmler, B. Neumann, U. Kölle, *Chem. Ber.* **1995**, *128*, 665; b) L. Weber, O. Sommer, H.-G. Stämmler, B. Neumann, *Z. Anorg. Allg. Chem.* **1996**, *622*, 543.
- [17] Holleman–Wiberg, *Lehrbuch der Anorganischen Chemie*, Walter de Gruyter, Berlin, **1995**, 997 and 1019.
- [18] T. Mohr, Thesis, University of Kaiserslautern, **1996**.
- [19] O. J. Scherer, J. Braun, G. Wolmershäuser, *Chem. Ber.* **1990**, *123*, 471.
- [20] G. L. Simon, L. F. Dahl, *J. Am. Chem. Soc.* **1973**, *95*, 2175.
- [21] O. J. Scherer, G. Kemény, G. Wolmershäuser, *Chem. Ber.* **1995**, *128*, 1145.
- [22] A. P. Ginsberg, W. E. Lindsell, K. J. McCullough, C. R. Sprinkle, A. J. Welch, *J. Am. Chem. Soc.* **1986**, *108*, 403.
- [23] S. A. Frith, J. L. Spencer, *Inorg. Synth.* **1985**, *23*, 15.
- [24] L. M. Cirjak, R. E. Ginsburg, L. F. Dahl, *Inorg. Chem.* **1982**, *21*, 940.